

UC Irvine

UC Irvine Previously Published Works

Title

Reductions in California's Urban Fossil Fuel CO2 Emissions During the COVID-19 Pandemic

Permalink

<https://escholarship.org/uc/item/7qm1p6bx>

Journal

AGU Advances, 3(6)

ISSN

2576-604X

Authors

Yañez, CC

Hopkins, FM

Xu, X

et al.

Publication Date

2022-12-01

DOI

10.1029/2022av000732

Copyright Information

This work is made available under the terms of a Creative Commons Attribution-NonCommercial-NoDerivatives License, available at

<https://creativecommons.org/licenses/by-nc-nd/4.0/>

Peer reviewed

Reductions in California's Urban Fossil Fuel CO₂ Emissions During the COVID-19 PandemicC. C. Yañez¹ , F. M. Hopkins² , X. Xu¹ , J. F. Tavares¹, A. Welch¹ , and C. I. Czimeczik¹ ¹Department of Earth System Science, University of California Irvine, Irvine, CA, USA, ²Department of Environmental Sciences, University of California Riverside, Riverside, CA, USA

Key Points:

- With COVID-19 restrictions, carbon dioxide (CO₂) levels on Los Angeles (LA) freeways were reduced by 119 ppm (or 60%) in July 2020 relative to 2019
- Plant radiocarbon analysis captured a 5 ppm reduction in LA fossil fuel CO₂ levels during the Stay-At-Home order
- Mobile and plant-based measurements of fossil fuel CO₂ can help quantify decarbonization progress in cities

Supporting Information:

Supporting Information may be found in the online version of this article.

Correspondence to:

C. C. Yañez and C. I. Czimeczik,
ccyanez@uci.edu;
czimeczik@uci.edu

Citation:

Yañez, C. C., Hopkins, F. M., Xu, X., Tavares, J. F., Welch, A., & Czimeczik, C. I. (2022). Reductions in California's urban fossil fuel CO₂ emissions during the COVID-19 pandemic. *AGU Advances*, 3, e2022AV000732. <https://doi.org/10.1029/2022AV000732>Received 26 APR 2022
Accepted 22 OCT 2022**Peer Review** The peer review history for this article is available as a PDF in the Supporting Information.

Author Contributions:

Conceptualization: C. C. Yañez, F. M. Hopkins, X. Xu, C. I. Czimeczik
Data curation: C. C. Yañez, X. Xu, J. F. Tavares, A. Welch
Formal analysis: C. C. Yañez, F. M. Hopkins, A. Welch, C. I. Czimeczik
Investigation: C. C. Yañez, F. M. Hopkins, X. Xu, C. I. Czimeczik

© 2022. The Authors.

This is an open access article under the terms of the [Creative Commons Attribution-NonCommercial-NoDerivs License](https://creativecommons.org/licenses/by/4.0/), which permits use and distribution in any medium, provided the original work is properly cited, the use is non-commercial and no modifications or adaptations are made.

Abstract Fossil fuel carbon dioxide (CO₂) emissions (ffCO₂) constitute the majority of greenhouse gas emissions and are the main determinant of global climate change. The COVID-19 pandemic caused wide-scale disruption to human activity and provided an opportunity to evaluate our capability to detect ffCO₂ emission reductions. Quantifying changes in ffCO₂ levels is especially challenging in cities, where climate mitigation policies are being implemented but local emissions lead to spatially and temporally complex atmospheric mixing ratios. Here, we assess ffCO₂ emission patterns associated with pandemic-induced changes to human activity using direct observations of on-road CO₂ mole fractions in the Los Angeles (LA) urban area and analyses of the radiocarbon (¹⁴C) content of annual grasses collected by community scientists throughout California, USA. With COVID-19 mobility restrictions in place in 2020, we observed a significant reduction in ffCO₂ levels across California, especially in urban centers. In LA, on-road CO₂ enhancements were 60 ± 16% lower than the corresponding period of 2019 and rebounded to pre-pandemic levels by 2021. Plant ¹⁴C analysis indicated ffCO₂ reductions of 5 ± 10 ppm in 2020 relative to pre-pandemic observations in LA. However, ffCO₂ emission trajectories varied substantially by region and sector as COVID-related restrictions were relaxed. Further development of these techniques could aid efforts to monitor decarbonization in cities, especially in developing countries without established CO₂ monitoring infrastructure.

Plain Language Summary Cities emit large amounts of greenhouse gases, especially fossil fuel-derived carbon dioxide (ffCO₂), and thus contribute to climate change. Reducing ffCO₂ emissions is challenging because it is difficult to quantify the many and variable ffCO₂ sources of individual neighborhoods and cities. Here, we measured ffCO₂ reductions during the COVID-19 pandemic, demonstrating that two measurement approaches are sensitive enough to detect changes in ffCO₂ at fine spatial scales. We measured CO₂ levels on Los Angeles freeways using a mobile laboratory and analyzed the radiocarbon content in plant species collected by community scientists across the state of California. Both analyses indicate substantial reductions in ffCO₂ emissions in 2020 during California's pandemic-related shift to remote work and varying degrees of emission rebounds by 2021. We found that measurements of radiocarbon in plants is particularly sensitive to local-scale changes in human activity. Our results demonstrate that measuring the radiocarbon content of plants can serve as a useful approach to quantify local changes in cities' ffCO₂ patterns and monitor decarbonization as climate agreements take effect. Further development and implementation of these methods could significantly improve our shared capacity to address climate change, particularly in cities in developing countries which often lack CO₂ monitoring infrastructure.

1. Introduction

Carbon dioxide (CO₂) emissions associated with fossil fuel consumption (ffCO₂) are the dominant cause of climate change (IPCC, 2022). Hence, there is an urgent need to quantify ffCO₂ emissions to support the success of climate change mitigation efforts. Urban areas account for 30%–84% of global ffCO₂ emissions (Seto et al., 2014), despite encompassing less than 1% of the Earth's land area (Zhou et al., 2015). While being disproportional contributors to climate change, cities are also at the forefront of climate change mitigation actions (Rosenzweig et al., 2010), making them a top priority for quantifying and monitoring ffCO₂ emission reduction efforts.

Satellite-borne instruments can detect CO₂ enhancements (i.e., 6 ppm above background) over large cities (Kiel et al., 2021; Schwandner et al., 2017), and urban tower networks continuously measure CO₂ levels in a small selection of cities in more economically developed countries. However, these atmospheric observation systems

Methodology: C. C. Yañez, F. M. Hopkins, X. Xu, C. I. Czimeczik
Project Administration: F. M. Hopkins, C. I. Czimeczik
Resources: C. C. Yañez, F. M. Hopkins, X. Xu, J. F. Tavares, A. Welch, C. I. Czimeczik
Supervision: F. M. Hopkins, C. I. Czimeczik
Validation: C. C. Yañez
Visualization: C. C. Yañez, A. Welch
Writing – original draft: C. C. Yañez
Writing – review & editing: C. C. Yañez, F. M. Hopkins, X. Xu, J. F. Tavares, A. Welch, C. I. Czimeczik

are limited in their ability to detect trends in ffCO₂ at the neighborhood scale (~1 km²) that is needed to inform local policy makers on the outcome of mitigation actions (Duren & Miller, 2012).

The abrupt halt of economic activity at the beginning of the coronavirus disease pandemic (COVID-19), with strictest regulations in place in the U.S. from March to May of 2020, provided an unplanned experiment on the sensitivity of atmospheric greenhouse gas (GHG) observations to changes in human behavior. Restrictions intended to prevent the spread of the virus caused a wide scale disruption of human activities and consequently the largest reduction in global ffCO₂ emissions than has ever been observed, inducing rapid emission reductions larger than any historical human crisis or climate agreement (Le Quéré et al., 2021). These emission reductions provide insight on potential climate mitigation strategies, such as decreasing transportation emissions through increased flexibility in remote work. Several studies quantified emission reductions during the pandemic using activity-based models (“bottom up” estimates) that scale sector-based activity and consumption data with CO₂ emission coefficients. One study calculated a 17% (11%–25%) reduction in daily global ffCO₂ emissions in April 2020 relative to 2019, based on a compilation of activity data and information on the intensity of mandated lockdowns (Le Quéré et al., 2020). Hourly to daily activity data indicated an overall global ffCO₂ decline of 8% in the first half of 2020 relative to 2019 (Liu et al., 2020).

Pandemic related emission reductions have also been assessed using atmospheric observations (“top-down” estimates). For instance, several cities have established in situ tower observation networks that continuously measure the total CO₂ mixing ratio. One such study reported a 30% reduction in the San Francisco Bay Area (SFBA)'s CO₂ levels during the first 6 weeks of California's statewide Stay-At-Home Order (March 22 to 4 May 2020) relative to the 6 weeks before the order (Turner, Kim, et al., 2020). Similar reductions were reported for the Los Angeles (34 ± 6%) and Washington DC/Baltimore metropolitan areas (33 ± 11%) in April 2020 relative to the previous two years (Yadav et al., 2021). Alternative ground-based atmospheric measurements were also used to assess ffCO₂ emission reductions during the pandemic. Strong reductions in CO₂ fluxes (−5 to −87%) were observed during lockdown periods relative to the same times in previous years in 11 European cities using eddy-covariance measurements of CO₂ exchange (Nicolini et al., 2022). Atmospheric oxygen measurements were applied as novel tracers for ffCO₂ emissions in the United Kingdom and detected a 23% (14%–32%) ffCO₂ reduction in 2020 annual emissions relative to a modeled scenario without the COVID-19 pandemic (Pickers et al., 2022).

Pandemic-related emission reductions were also observed in some remotely sensed data. One study combined bottom-up estimates and observations of nitrogen oxides (NO_x, pollutants that are co-emitted with CO₂ during fossil fuel combustion) from the Tropospheric Monitoring Instrument (TROPOMI) to calculate a 12% decline in China's CO₂ emissions in the first four months of 2020 relative to 2019 (Zheng et al., 2020). However, studies analyzing data from CO₂-observing satellites (such as OCO-2 and GOSAT) could not conclusively detect pandemic-related emission reductions because of sparse data retrievals, low resolution, and weak signals (Buchwitz et al., 2021; Chevallier et al., 2020).

Quantifying ffCO₂ emission reductions (i.e., isolating fossil fuel contributions from the total CO₂ signal) remains a key challenge for climate change mitigation efforts, especially at localized spatial scales. This is because ffCO₂ emissions are superimposed on large and poorly constrained fluxes from land ecosystems (e.g., photosynthesis and respirations of plants and soil microorganisms) that vary seasonally and interannually in response to temperature, the timing and amount of precipitation, drought, fire, plant life stage, and management (irrigation, harvest) as well as emissions from biofuel combustion and human metabolism (e.g., respiration, sewage). Recent work in the LA metropolitan area revealed that biospheric fluxes contribute a significant proportion (up to 30%) to the excess level of CO₂ observed in the urban atmosphere (Miller et al., 2020). Thus, an effective ffCO₂ monitoring system requires a direct way to isolate fossil fuel sources from other entangled CO₂ fluxes, high spatial resolution, and accessibility to global cities.

One high resolution, sector-specific approach is the deployment of mobile GHG observatories that map fine scale patterns in ffCO₂ emissions from vehicle sources on urban roads (Bush et al., 2015). Such mobile measurements offer distinct sensitivity to traffic-related ffCO₂ emissions since the signal is dominated by nearby vehicle emissions and ambiguity related to transported air mixtures from other sources is reduced. During the COVID-19 pandemic, one mobile study observed dramatic reductions in on-road enhancements of CO₂ (−41 ppm or a 63% reduction) relative to a period before lockdowns in Beijing, China (Liu et al., 2021).

Radiocarbon analysis of plants is another promising approach for quantifying urban ffCO₂ trends at the local scale. Radiocarbon (¹⁴C, a radioactive carbon isotope with a half-life of 5,730 years) is a unique tracer for ffCO₂ because fossil fuel-derived CO₂ is millions of years old and devoid of ¹⁴C due to radioactive decay, while other sources of CO₂ have ¹⁴C signatures similar to the current atmosphere (Graven et al., 2020; Levin et al., 2003; Turnbull et al., 2006). Currently, an input of 1 ppm of ffCO₂ into the atmosphere results in a depletion of ambient Δ¹⁴CO₂ by 2.4‰. Since plants assimilate CO₂ during photosynthesis, plant ¹⁴C reflects the ¹⁴CO₂ signature of the surrounding atmosphere integrated over the period when the plants are photosynthetically active. Where ffCO₂ emissions dilute ¹⁴C in the atmosphere, plants are depleted in ¹⁴C (appear older in ¹⁴C age). Thus, plants offer a natural and efficient network of ¹⁴C observations and can be used to map fine-scale spatial patterns in ffCO₂ in places without established CO₂ monitoring infrastructure (Hsueh et al., 2007; Riley et al., 2008; Santos et al., 2019; Wang & Pataki, 2010).

Several studies have measured the ¹⁴C of ambient air to quantify ffCO₂ trends in urban areas (Miller et al., 2020; Newman et al., 2016; Turnbull et al., 2011); however, plants offer time-integrated monitoring of ¹⁴C that could more feasibly be used to monitor ffCO₂ spatial patterns in global cities than deploying air sampling stations at the same scale. Preparation for ¹⁴C analysis is significantly faster for plant samples and can be done with just 4 mg of plant tissue since plants are approximately 40% C, while air samples (<0.04% C) require expensive canisters and larger volume samples (approximately 5 L) and longer processing times to get a large enough ¹⁴C sample for AMS analysis. This means that more ¹⁴C samples can be analyzed leading to higher spatial resolution urban ffCO₂ datasets than with air samples. During COVID-19 lockdowns in New Zealand, the ¹⁴C of weekly-sampled grasses tracked changes in local ffCO₂ emissions that coincided with the stringency of COVID-related restrictions and detected a 75% ± 3 peak reduction in ffCO₂ emissions (Turnbull et al., 2022).

Here, we quantify changes in ffCO₂ emissions during select periods of the COVID-19 pandemic (spring and summer of 2020 and 2021) in California, USA, with a focus on the state's two largest urban areas: the LA metropolitan area and the SFBA. The State of California is the world's fifth largest economy (based on the state's GDP of 3.36 trillion USD in 2021, [bea.gov](https://www.bea.gov)) and has enacted landmark climate action legislation. Statewide policies that restricted mobility likely altered ffCO₂ emission patterns during the pandemic, such as the Stay-At-Home order that required the closing of all “non-essential” businesses from 19 March to 4 May 2020 (Executive Order N-33-20). To examine the impacts of these policies on ffCO₂ emissions, we use two approaches that can isolate CO₂ derived from fossil sources, are spatially resolved, and do not require establishment of CO₂ monitoring infrastructure. First, we measured the mixing ratio of CO₂ on freeways in the LA area using a mobile GHG observatory. Second, we analyzed the ¹⁴C content of annual grasses collected by community scientists across the state. Together, our data offer a unique insight into anthropogenic ffCO₂ emissions in California's urban regions during the COVID-19 pandemic and support the further use of plant ¹⁴C analysis to evaluate decarbonization efforts in other cities.

2. Methods

2.1. On-Road CO₂ Measurements

We measured the on-road mixing ratios of CO₂ in the LA metropolitan area using a cavity ringdown spectrometer (G2401, Picarro) installed inside a mobile laboratory (2016 Mercedes Sprinter cargo van). The same platform has been used by previous studies to observe GHG and pollutant concentrations (Carranza et al., 2022; Thiruvankatachari et al., 2020). Ambient air was continuously pumped into the Picarro from an inlet on the roof of the van behind the driver's seat, approximately 3 m above the road surface. We simultaneously collected position and meteorological data using a global satellite positioning device (GPS 16X, Garmin) and a compact weather sensor (METSSENS500, Campbell Scientific) that were mounted on the roof of the vehicle.

Measurements were collected on freeways during daytime hours on weekdays in July 2019, 2020, and 2021. We filtered the datasets from each year to only include locations that overlapped with the 2020 data set, focusing the analysis on approximately 750 km of road. To minimize meteorological effects on our results, we only used data collected between 11 a.m. and 4 p.m. local time, when the planetary boundary layer is well-developed and surface layer air is well-mixed (Ware et al., 2016). These times exclude typical rush hour traffic periods and make our analysis conservative since rush hour emissions were likely the most strongly reduced in 2020 as commuters switched to working from home. We also filtered out data from days that were overcast and otherwise

experienced similar weather conditions during all three surveys. Different filtering strategies would be required for cities that experience different meteorology than LA.

We calibrated the analyzer before and after each survey using gas cylinders with CO₂ mixing ratios that have been corrected against the NOAA WMO-CO₂-X2007 scale. For each calibration, the analyzer inlet was directed to sample air from compressed gas cylinders with known mixing ratios of CO₂ for 3 minutes. We used two standard tanks that spanned the range of CO₂ mixing ratios we observed on the road (Table S1 in Supporting Information S1). We then applied a two-point correction to the data based on the linear relationship between the known and measured values. The measurements are precise to <1 ppm for all surveys based on the standard deviation of the calibration runs. The calibrated data was aggregated into 5-s intervals and gridded into 100-m road segments to synchronize trace gas, weather, and position measurements.

Urban CO₂ enhancements (CO_{2xs}) were calculated by subtracting a background that represents the CO₂ mole fraction of air coming into the LA area before it is enhanced by local emissions. For urban studies, background characterization generally depends on latitude, seasonal wind patterns, and topography. Previous studies in other cities have used CO₂ measurements from upwind rural areas or a high elevation site to represent the background (Mitchell et al., 2018; Turnbull et al., 2018). Since westerlies prevail in LA in July, a suitable background can be represented by the inflowing marine air that originates in the Pacific Ocean (Newman et al., 2016; Verhulst et al., 2017). Thus, we characterized the CO₂ background using flask sample data from NOAA's Global Monitoring Division's site at Cape Kumukahi, Hawaii (19.54°N, 154.82°W, 15 m elevation). The NOAA GMD data is publicly available at <https://gml.noaa.gov/> (Dlugokencky et al., 2021), and hosts a network of over 50 sites that monitor trace gas concentrations around the world. Previous work has found that Cape Kumukahi's CO₂ levels are similar to the local LA background for summer months (Hopkins et al., 2016). Based on the July average of all flask measurements at Cape Kumukahi, we estimate the CO₂ background was 411.0 ± 2.0 ppm in 2019, 412.9 ± 1.2 ppm in 2020, and 416.7 ± 1.7 ppm in 2021. On 31 July 2020, we measured similar CO₂ mixing ratios (413 ± 1.4 ppm) in the in-flowing marine air at Dockweiler Beach (33.94°N, -118.44°E), which supports the application of Cape Kumukahi as an adequate LA background.

We assume that the observed CO₂ enhancements are solely derived from on-road emissions. It is possible that some of these enhancements are influenced by biosphere fluxes and wildfire emissions. However, we expect that these contributions are relatively small and do not affect the results.

2.2. Radiocarbon Analysis of Plants

We measured the ¹⁴C content of invasive annual grasses to map ffCO₂ trends across the state of California. The typical growing season of these species lasts from March to May, which coincided with California's statewide Stay-At-Home Order (March 19 to 4 May 2020) and made them useful bio-monitors of fossil fuel emission-reductions during the period of strictest COVID-19 measures in this area.

Because plant ¹⁴C reflects the CO₂ assimilated from the atmosphere during photosynthesis, differences in ¹⁴C depletion between plant samples are driven by local differences in ambient ¹⁴CO₂ composition and particularly the amount of fossil fuel influence. Studies around the world have mapped ffCO₂ patterns using a variety of plant species appropriate for their study area including tree rings in LA (e.g., Djuricin et al., 2012), evergreen tree leaves in Italy (Alessio et al., 2002), corn leaves in the United States (Hsueh et al., 2007) and Beijing, China (Xi et al., 2011), annual grasses in California (Riley et al., 2008; Wang & Pataki, 2010), ipê leaves in Rio de Janeiro (Santos et al., 2019), turfgrasses in New Zealand (Turnbull et al., 2022), and wheat crops in India (Sharma et al., 2023). Thus, cities can apply this technique to quantify ffCO₂ patterns by sampling a commonly found plant species that is photosynthetically active during the time integration period of interest. Unlike stable isotope signatures, plant ¹⁴C content does not vary based on photosynthetic pathway, water use efficiency or other growth factors. Such factors are corrected for since the measured plant ¹⁴C/¹²C ratios are normalized to a δ¹³C value of -25‰. Other than fossil fuel influence, the biggest drivers of ¹⁴C differences between plant species would be from the usage of stored carbon in perennial plants (Vargas et al., 2009) and from local topographic conditions (i.e., photosynthetic fixation of soil-respired CO₂ in depressions).

We recruited community scientists to collect plant samples from their neighborhoods. We distributed a packet that contained scientific background information, sampling/mauling instructions, and photos to aid with plant identification. We also held informational webinars, gave presentations at community college classrooms, and

uploaded videos online demonstrating how to collect and mail the samples. Nearly 400 plant samples were submitted for the study. Most samples were collected on residential properties or along roadsides in public areas. The plant samples were mailed in paper envelopes along with the species, latitude, longitude, and date of collection. Collection dates for the samples ranged from late spring through the summer. Most plants were *Bromus tectorum* L. (cheatgrass), *Bromus diandrus* Roth. (ripgut brome), *Avena fatua* L. (wild oat), or *Avena barbata* POTT EX LINK (slender oat). We inventoried all samples and information, confirmed their species (if identifiable), and recorded whether they were green or senesced. We also photographed all samples, focusing on their identifying features. These species represent a lower limit on annual ffCO₂ values since their growth period follows winter rain and wind events that cleanse pollution from the atmosphere.

We analyzed the ¹⁴C content of 188 samples from the 2020 growing season and 82 samples from the 2021 growing season. We excluded plants that were not annual species, did not contain flowers, and any that showed signs of decay (rot, mold). We prioritized analysis of samples that were expected to have high ffCO₂ signals (urban areas) and were collected at similar locations in both years. To prepare the samples for ¹⁴C analysis, we weighed out approximately 4 mg of plant tissue, focusing on flowers to target carbon fixed from the atmosphere during March to May. Samples were sealed into pre-combusted quartz tubes with cuprous oxide, which were then evacuated and combusted at 900°C for 3 hr. The resulting CO₂ was purified cryogenically on a vacuum line, quantified manometrically, and converted to graphite using a sealed-tube zinc reduction method (Xu et al., 2007). The graphite was analyzed for ¹⁴C at the W. M. Keck Carbon Cycle Accelerator Mass Spectrometer facility (NEC 0.5MV 1.5SDH-2 AMS) at the University of California, Irvine alongside processing standards and blanks. The measurement uncertainty ranged from 1.4 to 2.1‰. We use the Δ¹⁴C notation (‰) for presentation of results (Equation 1),

$$\Delta^{14}\text{C} = 1000 \cdot \left(\text{FM} \cdot \exp\left(\frac{1950 - y}{8267}\right) - 1 \right) \quad (1)$$

where y is the year of sampling, FM is the fraction modern calculated as the ¹⁴C/¹²C ratio of the sample divided by 95% of the ¹⁴C/¹²C ratio of the oxalic acid (OX) I standard measured in 1950, 8,267 years is the mean lifetime of ¹⁴C, and 1950 is the reference year for “modern.” Mass-dependent isotopic fractionation of the sample is accounted for in the fraction modern term (Trumbore et al., 2016). This ¹⁴C notation includes a correction for the decay of the OX I standard since 1950, giving the absolute ¹⁴C content of our samples during the year they were collected.

We used a mass balance approach (Santos et al., 2019; Turnbull et al., 2011) to quantify the fossil fuel contribution to the local CO₂ signal (C_{ff}) at each sample location. In the following equations, C_i terms denote CO₂ mixing ratios (units of ppm) from each contributing source and Δ_i terms denote the corresponding ¹⁴C signature for each source in units of per mil (‰).

$$C_{\text{obs}} \cong C_{\text{bg}} + C_{\text{ff}} \quad (2)$$

$$C_{\text{obs}}\Delta_{\text{obs}} \cong C_{\text{bg}}\Delta_{\text{bg}} + C_{\text{ff}}\Delta_{\text{ff}} \quad (3)$$

$$C_{\text{ff}} \cong C_{\text{bg}} \frac{(\Delta_{\text{bg}} - \Delta_{\text{obs}})}{(\Delta_{\text{obs}} - \Delta_{\text{ff}})} \quad (4)$$

Here, we assume the observed mixing ratio of CO₂ (units of ppm) at a location is the sum of two contributions: the CO₂ background (C_{bg}) and a fossil fuel contribution (C_{ff}) (Equation 2). The isoproduct for each CO₂ source must also be conserved (Equation 3). Combining Equations 2 and 3, we can calculate C_{ff} for each sample (Equation 4). All other values are known: Δ_{obs} is the measured ¹⁴C content of the plant sample. For C_{bg} we use the average CO₂ mixing ratio measured at Cape Kumukahi (Dlugokencky et al., 2021) between March and May. C_{bg} was 416.7 ± 1.1 ppm for the 2020 and 419.4 ± 0.8 ppm for the 2021 growing season, respectively. The Δ¹⁴C of background air (Δ_{bg}) is characterized by monthly-integrated air samples collected in a remote location Pt. Barrow, Alaska (X. Xu, Pers. Comm., 2021) and was -2.8 ± 1.3 ‰ for the 2020 and -6.2 ± 1.7 ‰ for the 2021 growing season, respectively. Δ_{ff} is $-1,000$ ‰, the known fossil fuel ¹⁴C signature. Based on the average standard deviation of replicate plant samples and error propagation of the measurement uncertainty, the uncertainty in a C_{ff} estimate is 1 ppm. Our equations assume biogenic ¹⁴C inputs (such as from fires or heterotrophic respiration) are small enough to be neglected in the mass balance budget. Previous work has shown that this effect is constant

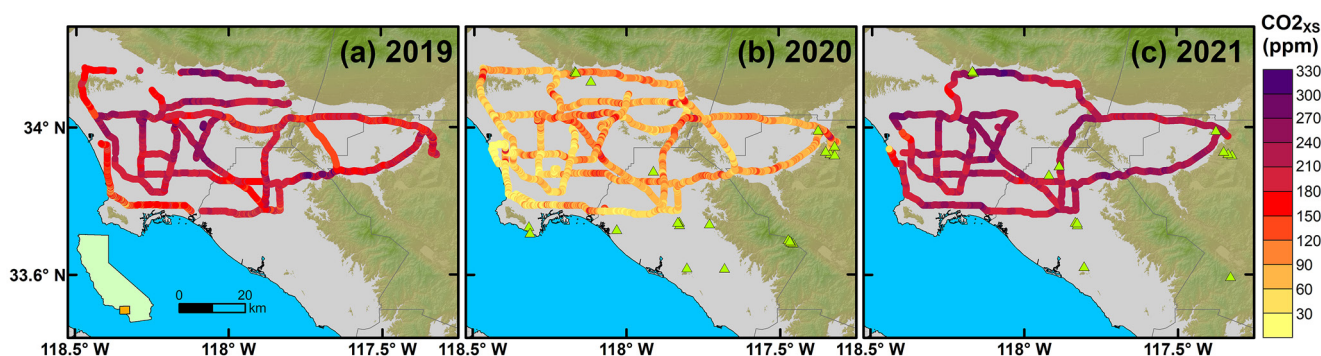


Figure 1. On-road $\text{CO}_{2\text{xs}}$ observed near midday on Los Angeles freeways before (2019) and during the COVID-19 pandemic (2020 and 2021). Choropleth maps show $\text{CO}_{2\text{xs}}$ observations in (a) July 2019, (b) July 2020, and (c) July 2021. Green triangles show locations of plant ^{14}C samples collected in 2020 and 2021. Basemap shows topography for elevations >300 m as hillside shading based on a Digital Elevation Model from USGS.

and relatively small (Newman et al., 2016). The plant growing season (March to May) is outside of California's wildfire season, so we do not expect wildfire emissions to affect the plant ^{14}C signatures. We also assume that the samples were not affected by ^{14}C emissions from nuclear power plants since there is only one such facility that is active in California (the Diablo Canyon Power Plant in San Luis Obispo County). The nearest plant sample was approximately 17 km northeast of the facility, which is not in the path of the area's dominant wind direction and is likely too far to intercept the emissions.

We expect that meteorology had minimal impact on our ^{14}C analysis since the plant samples experienced similar meteorological conditions across both study years, and because our plants only assimilate CO_2 during daytime hours. Thus, sampling excludes periods of strong atmospheric stability such as nighttime and early mornings which have increased CO_2 levels that are not driven by changes in ffCO_2 emissions (Djuricin et al., 2012; Newman et al., 2016; Verhulst et al., 2017).

3. Results and Discussion

3.1. Reduced CO_2 Enhancements on Los Angeles Freeways

We observed substantial reductions in on-road CO_2 enhancements ($\text{CO}_{2\text{xs}}$) in the LA metropolitan area during the pandemic (Figure 1). The mean $\text{CO}_{2\text{xs}}$ value ($\pm\text{SD}$) on LA freeways was 119 ± 50 ppm lower in July 2020 compared to July 2019 (Table 1), a $-60 \pm 16\%$ change with $\text{CO}_{2\text{xs}}$ reductions observed universally across all sampled freeways. By July 2021, COVID-related changes in behavior were reduced and $\text{CO}_{2\text{xs}}$ rebounded by 153 ± 40 ppm compared to 2020 (Table 1). This equates to a $17 \pm 29\%$ increase in $\text{CO}_{2\text{xs}}$ levels in July 2021 relative to July 2019. The 2021 $\text{CO}_{2\text{xs}}$ increases were not uniformly distributed. Many freeways still had $\text{CO}_{2\text{xs}}$ values that were lower relative to 2019, although not nearly as low as in 2020. Heavily trafficked areas had $\text{CO}_{2\text{xs}}$ levels as much as 40% higher than 2019 (Figure S1 in Supporting Information S1). Furthermore, $\text{CO}_{2\text{xs}}$ values were less variable in 2020 (interquartile range of 33 ppm) and 2021 (interquartile range of 43 ppm) compared to 2019 (58 ppm), indicating more homogeneous $\text{CO}_{2\text{xs}}$ on roadways during the pandemic (Figure S2 in Supporting Information S1).

Changes in traffic patterns during the pandemic are likely the main cause of the changes in on-road $\text{CO}_{2\text{xs}}$ values we observed. In addition to the number of cars on road, previous work has shown that on-road CO_2 mixing ratios are sensitive to traffic conditions such as speed, distance between cars and road grade (Maness et al., 2015). In July 2020, schools and businesses were operating in a remote or hybrid work model and many commercial facilities were closed, leading to substantial traffic reductions. Data from the California Department of Transportation's Performance Measurement System indicates that the vehicle miles traveled (VMT) on Southern California freeways was on average 12% lower in July 2020 compared to July 2019 (Caltrans, 2021). With fewer vehicles on the road in July 2020, there were wider distances between cars, fewer traffic jams, and fewer CO_2 emissions.

Nationwide studies conducted during the same period deduced that ffCO_2 emissions started recovering after reaching minima in March or April of 2020, and that by July of 2020 (our study period), the reductions had largely diminished (Harkins et al., 2021; Le Quéré et al., 2020; Liu et al., 2020). Daily ground transportation emissions

Table 1
Changes in ffCO₂ Levels During the COVID-19 Pandemic in California Based on on-Road Mobile Surveys and Observations of ¹⁴C in Plants And/or Air

Region	Pre-pandemic	2020	2021	COVID-19 ^a	Rebound ^b
CO _{2xs} (ppm) via on-road mobile surveys					
LA	199 ± 42 ^c	80 ± 27	233 ± 29	-119 ± 50*	153 ± 40*
ffCO ₂ (ppm) based on ¹⁴ C in plants and/or air					
CA	4 ± 5 ^d	4 ± 4	5 ± 5	0 ± 6	1 ± 6
<i>co-located</i>	<i>n.a.</i>	5 ± 5	5 ± 6	<i>n.a.</i>	0 ± 8
LA	11 ± 9 ^e	6 ± 5	9 ± 7	-5 ± 10*	3 ± 9
<i>co-located</i>	<i>n.a.</i>	9 ± 9	11 ± 10	<i>n.a.</i>	2 ± 13
Pasadena	23 ± 4 ^f	3	13 ± 2	-20 ± 4*	10 ± 2*
Irvine	7 ± 4 ^g	6	4 ± 1	-1 ± 4	-2 ± 1

Note. Asterisk (*) indicates the means were significantly different based on Welch's *t*-test. Further details for these calculations are in Table S2 in Supporting Information S1. Uncertainties are standard deviations. Values that do not have uncertainties indicate a sample size of 1. For these cases, the uncertainty in the ffCO₂ estimate is assumed to be 1 ppm based on the differences in replicated plant samples. Values in regular font represent all the samples collected in that year, while values in italicized font represent only co-located plant samples that were collected in both 2020 and 2021 less than 150 m apart.

^aCalculated as the difference between the 2020 (intense physical distancing measures and mobility restrictions) and pre-pandemic columns. The pre-pandemic observations are based on datasets from various years and are described in the subsequent footnotes and Table S2 in Supporting Information S1. ^bCalculated as the difference between 2021 and 2020 (relaxation of physical distancing measures and mobility restrictions). ^cJuly 2019 on-road mobile measurements. ^d2005 plant ¹⁴C observations (Riley et al., 2008). ^eBased on 2005 plant ¹⁴C observations (Wang & Pataki, 2010) and 2015–2016 air ¹⁴C samples (Miller et al., 2020). ^fPredicted 2020 value based on a linear extrapolation of 2006–2013 air ¹⁴C samples (Newman et al., 2016) assuming the trend continued and there had been no pandemic. ^g2019 air ¹⁴C samples (Xu, pers. Comm., 2020).

in the U.S. were estimated to only be reduced by 7%–8% in July 2020 compared to 2019 (Harkins et al., 2021; Liu et al., 2020). Interestingly, our LA observations indicate much larger reductions to on-road CO₂ emissions during that period (~60%). This is likely because our measurements were collected in an area where emissions are dominated by passenger vehicles. In California and in LA, the transportation sector is the largest source of ffCO₂ emissions (45% of total), so changes in traffic patterns during the pandemic were more likely to have a discernible impact on this region's ffCO₂ budget. A 60% decrease in on-road emissions is consistent with a previous estimate that the LA area's total emissions were reduced by 30% in the spring of 2020 relative to 2018–2019 (Yadav et al., 2021). A budget balance calculation with a 30% reduction in total LA emissions in 2020 equates to a 67% reduction in on-road emissions if we assume non-vehicle ffCO₂ sources were held constant and the on-road sector accounted for 45% of LA's ffCO₂ emissions before the pandemic. However, previous studies have shown that the pandemic-related emission reductions are not completely attributable to changes in traffic (Liu et al., 2020; Yadav et al., 2021), so our ~60% reduction result is still higher than what other studies estimated. On-road CO₂ measurements are likely to detect the transportation-sector emission changes with higher sensitivity than tower- and space-based observations since signal detection is not as dependent on atmospheric transport.

While our data revealed striking reductions in CO₂ mixing ratios, it is not trivial to translate changes in on-road CO₂ mixing ratios into reductions in CO₂ emissions. One reason for this is confounding effects of changes in vehicle speeds on CO₂ emissions. There is a nonlinear relationship between vehicle speeds and emission rates, such that vehicles emit more CO₂ at very low and very high speeds (Fitzmaurice et al., 2022). In 2020, our average speed was 9 km hr⁻¹ faster than 2019 and 12 km hr⁻¹ faster than 2021, which suggests a decrease in congestion in 2020. Within the range of our average speeds (64–76 km/hr), there is not expected to be a substantial change in CO₂ emission rates (Fitzmaurice et al., 2022). However, these averages do not capture the non-constant speeds during periods of congestion that make vehicles less efficient and increase both CO₂ emissions (Barth & Boriboonsomsin, 2008) and roadway enhancements. Faster speeds produce more CO₂ emissions because vehicle engines are doing more work and using more fuel, but they also create more turbulence near the road that effectively mixes vehicle emissions, thereby reducing on-road CO₂ enhancements. Nonetheless, we did not find a significant relationship between our measurements of CO_{2xs} and vehicle speed (Figure S3 in

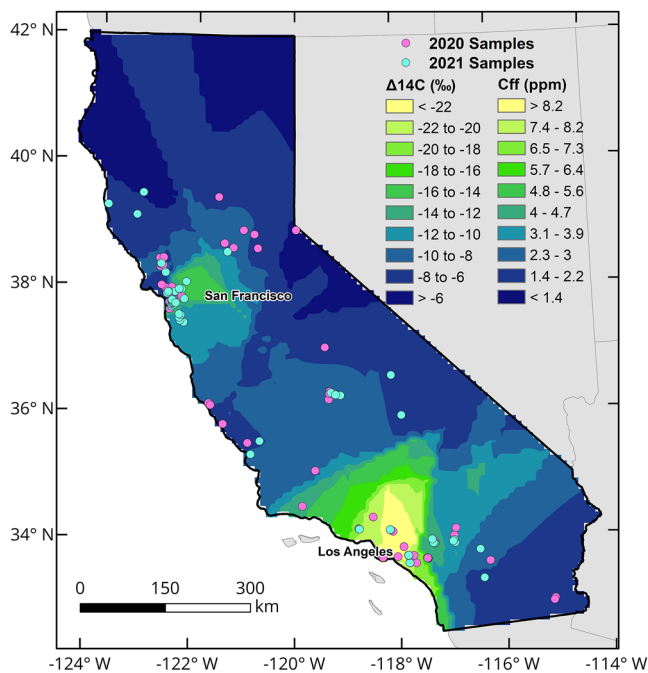


Figure 2. The $\Delta^{14}\text{C}$ (‰) of annual grass samples collected in California, USA and the corresponding C_{ff} values in 2020. Blue points indicate locations where plants were collected in both 2020 and 2021, while pink points indicate 2020-only locations. Background colors were mapped using an ordinary kriging interpolation of 2020 plant $\Delta^{14}\text{C}$ values using the Spatial Analyst toolbox in ESRI's ArcMap software. The uncertainty in the kriging prediction is presented in Figure S4 in Supporting Information S1.

Supporting Information S1). We estimated how much vehicle speed would affect our measurements using a model where on-road $\text{CO}_{2\text{xs}}$ levels scale with vehicle speed to a power of $-1/3$ (Baker, 1996; Maness et al., 2015). Assuming that total highway emissions (Q) are related to $\text{CO}_{2\text{xs}}$ and vehicle speed (v) by Equation 5 where κ is a constant of proportionality based on theoretical atmosphere and traffic conditions, a 9 km/hr increase in speed as observed in 2020 only causes total emissions to increase by less than 5%. Thus, we attribute the measured $\text{CO}_{2\text{xs}}$ reductions to the smaller number of cars on the road, not the changes in speed.

$$\text{CO}_{2\text{xs}} = \kappa Q v^{-1/3} \quad (5)$$

Interestingly, our on-road observations did not scale proportionally with vehicle miles traveled (VMT), a metric that has been used to infer ffCO_2 emissions from the transportation sector (Gately et al., 2015; Gurney et al., 2020). While we observed a $60 \pm 16\%$ reduction in $\text{CO}_{2\text{xs}}$ in July 2020 relative to July 2019, VMT in the LA area was only reduced by 12% during the same time periods (Caltrans, 2021). VMT does not adequately capture the strong CO_2 signal we observed because it does not account for the effects of driving behavior, congestion, vehicle speeds, and fleet composition on CO_2 emissions (Rao et al., 2017), all of which likely changed during 2020. While relationships between emissions and speed are incorporated in some models, less work has incorporated the effects of stop-and-go driving, which is likely to produce higher CO_2 emissions. Less congestion in 2020 could have reduced CO_2 emissions in ways that have not been fully explored. Other studies also reported large discrepancies between ffCO_2 emission estimates based on governmental traffic data, fuel-based models, and novel cell phone-based mobility datasets (Gensheimer et al., 2021; Harkins et al., 2021; Oda et al., 2021). Future work is needed to consolidate these different metrics for estimating transportation ffCO_2 emissions and to better understand what information each of these datasets represents.

Assuming the measured 60% reduction in on-road $\text{CO}_{2\text{xs}}$ translates into a 60% reduction in annual interstate ffCO_2 emissions (7.6 Mt C yr^{-1} in 2012; Rao et al., 2017), given that interstates are the primary road type included in this analysis, this equates to an avoided 4.6 Mt C . The estimated total emissions for the LA area was $47.2 \pm 5.2 \text{ Mt C yr}^{-1}$ in 2015 (Gurney et al., 2019). This would imply that LA's total ffCO_2 emissions were reduced by 10% if all the pandemic-induced reductions in 2020 were solely due to changes to on-road interstate emissions (neglecting ffCO_2 changes in other sectors, such as residential, industry, and non-interstate roads). Interstate emissions constitute only 40% of LA's on-road emissions (Rao et al., 2017). If we instead assume the COVID-induced traffic reductions resulted in a 60% reduction in ffCO_2 for the entire on-road sector (including all road types), then ffCO_2 emissions were reduced by 11.4 Mt C , or 24% of LA's total ffCO_2 emissions.

3.2. Reduced ffCO_2 Emissions During the Stay-At-Home Order

^{14}C analyses of plant species were used to map ffCO_2 patterns, whereby lower $\Delta^{14}\text{C}$ values indicate higher ffCO_2 inputs (Figure 2). In 2020, the average $\Delta^{14}\text{C}$ ($\pm\text{SD}$) was $-11.3 \pm 8.6\text{‰}$ ($n = 188$) statewide, and $-15.9 \pm 12.5\text{‰}$ ($n = 53$) in the LA area, $-10.2 \pm 5.5\text{‰}$ ($n = 91$) in the SFBA, and $-10.3 \pm 5.6\text{‰}$ ($n = 12$) in the San Joaquin Valley. This equates (Equation 4) to average fossil fuel contributions of $4 \pm 5 \text{ ppm}$ statewide, and $6 \pm 5 \text{ ppm}$ in the LA area, $3 \pm 2 \text{ ppm}$ in the SFBA, and $3 \pm 2 \text{ ppm}$ in the San Joaquin Valley. The cleanest samples were found in California's northern coast ($\Delta^{14}\text{C}$ of $-5.3 \pm 3.7\text{‰}$, $n = 5$). Generally, $\Delta^{14}\text{C}$ of plants collected in urban areas were more depleted and more variable than in non-urbanized regions, indicating higher and locally variable emissions of ffCO_2 (Figure 2). Sample collection was biased toward urban areas, with 77% of samples collected either in the LA area or SFBA, leading to higher uncertainty in predictions in other regions of the state (Figure S4 in Supporting Information S1). However, we expect rural and remote areas such as northern California and the Sierra Nevada Mountains to have similar ^{14}C values as the background and little variability (Riley

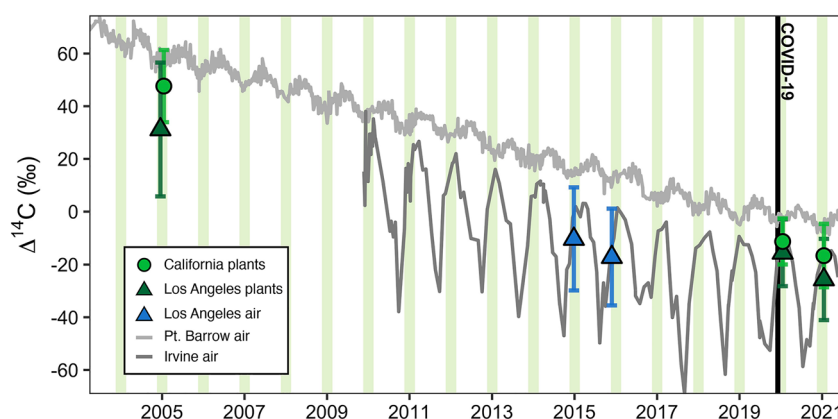


Figure 3. A record of $\Delta^{14}\text{C}$ measurements from 2003 to 2021. Average plant ^{14}C from various studies are shown as green points with error bars showing the standard deviation. Green circles represent statewide data (this study and Riley et al., 2008) while triangles represent only the Los Angeles metropolitan area (this study and Wang & Pataki, 2010). Air-based ^{14}C observations are shown as gray lines (X. Xu, Pers. Comm., 2021) and blue triangles (Miller et al., 2020). Shaded green bars represent the typical annual grass growing season in California (March to May).

et al., 2008). Thus, while we do not have a lot of plant samples in these areas, we do not expect to see substantial COVID-effects on ffCO_2 levels.

To assess our 2020 plant ^{14}C observations in the context of long-term trends in the region, we compared our data to existing records of ^{14}C in plants and/or air from Irvine, CA (a coastal city south of LA) and Pt. Barrow, AK (a remote location far from ffCO_2 sources) (Figure 3).

We infer urban ffCO_2 emission reductions during the 2020 Stay-At-Home order relative to the ^{14}C records shown in Figure 3 based on two metrics: variability in ^{14}C (standard deviation of mean) and the difference in ^{14}C from the hemispheric background (Pt. Barrow, Alaska). Reduced variability in ^{14}C indicates reduced ffCO_2 levels since emissions lead to anomalous and spatially variable ^{14}C values. The standard deviations of plant $\Delta^{14}\text{C}$ samples collected in the LA metropolitan area were 25.4‰ in 2005 ($n = 79$, Wang & Pataki, 2010), 12.5‰ in 2020 ($n = 53$), and 15.4‰ in 2021 ($n = 27$). Thus, plant ^{14}C was less variable during California's 2020 Stay-At-Home order.

Furthermore, 2020 samples were more similar to the hemispheric background than in other years. Compared to Pt. Barrow, samples collected in the LA area were depleted in ^{14}C by $26 \pm 3\text{‰}$ in 2005 (plant samples; Wang & Pataki, 2010), $25 \pm 2\text{‰}$ in 2015, $30 \pm 4\text{‰}$ in 2016 (flask samples; Miller et al., 2020), $13 \pm 2\text{‰}$ in 2020, and $19 \pm 3\text{‰}$ in 2021 (this study's plant samples; average depletion \pm standard error of the mean). The mean 2020 depletion is significantly smaller than pre-pandemic years to a 95% confidence interval, indicating that ffCO_2 levels were reduced in 2020. Translating the ^{14}C depletion from background into fossil fuel-sourced CO_2 enhancements (Equation 4), the mean C_{ff} in LA during pre-pandemic years ranged from 10 to 13 ppm (Table S2 in Supporting Information S1). However, during the pandemic the mean C_{ff} reduced to 6 ± 5 ppm (Table 1). Thus, we calculate ffCO_2 levels were reduced by 5 ± 10 ppm relative to pre-pandemic observations.

These samples reflect varying locations within the Los Angeles region, and hence we are assuming that both prior and current plant samples as well as previous flask samples are similarly representative of the region. To minimize the impact of these assumptions, we also estimated ffCO_2 emission reductions in one location, Pasadena, a city in the northeast LA basin that receives polluted air from the LA region during afternoon hours (Newman et al., 2008). Based on a linear extrapolation of the Pasadena air record (Newman et al., 2016), the mean $\Delta^{14}\text{C}$ during the 2020 growing season (March to May) would have been $-55.5 \pm 8.8\text{‰}$ had there been no pandemic, translating to a local enhancement of 23 ± 4 ppm CO_2 above background (Equation 4). However, a plant sample collected in 2020 approximately 4 km away had an enhancement of only 3 ± 1 ppm CO_2 (Figure 4). This difference indicates a reduction of 20 ± 4 ppm ffCO_2 in Pasadena during the 2020 Stay-At-Home order. In 2021, plants were sampled in this location again and had an average $\Delta^{14}\text{C}$ of $-35.7 \pm 4.5\text{‰}$ ($n = 6$), an enhancement of 13 ± 2 ppm CO_2 . This value is closer to, but still significantly different from, the predicted 2021 mean value

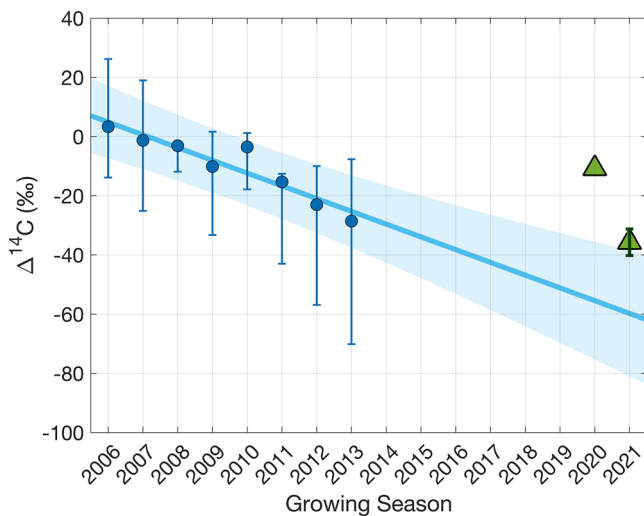


Figure 4. Growing season $\Delta^{14}\text{C}$ of ambient CO_2 in Pasadena, CA, a city within the northeast Los Angeles basin. The blue circles show the average growing season (March to May) $\Delta^{14}\text{C}$ of ambient CO_2 at Caltech (Newman et al., 2016), with error bars showing the minimum and maximum $\Delta^{14}\text{C}$ measurements. The line is a linear regression of these data with shading indicating the 95% confidence intervals. The green triangles show the measured $\Delta^{14}\text{C}$ of plant samples collected approximately 4 km away from the Caltech site in 2020 ($n = 1$) and 2021 ($n = 6$, error bars show standard deviation).

($-60 \pm 9.4\%$ or 24 ± 5 ppm CO_2 enhancement), indicating a partial but not complete rebound to the pre-pandemic emissions trend. Thus, plant ^{14}C data captured interannual changes in local ffCO_2 during the pandemic.

3.3. Changes in ffCO_2 During the Rebound Period (2020–2021)

Although the pandemic continued into the 2021 growing season, virus-restricting mandates were relaxed and California's VMT were 30% higher than the same period in 2020 (Caltrans, 2021). We observed large spatial variations and heterogeneity in ^{14}C during the second spring of the pandemic. Based on a subset of samples collected at similar locations (<150 m away) in both 2020 and 2021, we find that ffCO_2 levels did not change significantly between 2020 and 2021 at the statewide scale, with a mean change of 0 ± 8 ppm (Table 1). This average belies significant local variability in changes in $\Delta^{14}\text{C}$ between 2020 and 2021 (Figure S5 in Supporting Information S1). The disparity in ffCO_2 emission rebounds in 2021 could be related to variations in pandemic responses as the economy recovered after the Stay-At-Home Order. We observed larger emission rebounds in LA than SFBA (Figure 5 and Figure S6 in Supporting Information S1). SFBA had more instances of $\Delta^{14}\text{C}$ values that either increased or only decreased as much as the long-term global ^{14}C trend between 2020 and 2021. The SFBA had a slower relaxation of COVID-19 prevention measures than other regions of California. Here, and also in Orange County in the LA area, many people continued to work from home into 2021, which may explain why emission reductions generally persisted even after lockdown restrictions were lifted (blue areas in Figures 5a and 5b). In LA neighborhoods, working from home was not an option for many “essential” workers, which might contribute to

samples showing a stronger emission rebound in 2021 (red areas in Figure 5b). These neighborhoods also have a greater density of freeways.

We used city land use data to further investigate the ffCO_2 emission sectors represented by plant samples collected in the LA area and SFBA (45 sample pairs, Figure 5c). We found that the majority of plants were collected in areas classified as residential (58% of paired samples) or open space/recreation (29%). While there is large variation in ^{14}C within each category and results indicate that heterogeneity within regions/sectors was larger than the COVID-induced changes, there is a small trend toward higher ffCO_2 emissions in residential, open space/recreation and industrial areas, and a trend toward lower emissions from educational and public spaces. This is consistent with a return to normal of many activities, whereas schools in California stayed closed through the 2021 growing season and many government sector employees continued work from home. These sector-averaged trends are larger when all data is used (Figure S7 in Supporting Information S1) but are on the order of ± 1 –2 ppm, which is not much larger than the uncertainty in our C_{ff} estimates (± 1 ppm).

The heterogeneity in year-to-year changes elucidates the highly localized sensitivity of plant ^{14}C and indicates that this approach is a simple, yet effective method to monitor interannual changes in the ffCO_2 burden at the neighborhood scale. This approach is most effective at tracking changes in local emissions if plants are periodically collected in direct proximity (<20 m) from ffCO_2 emission sources. For instance, the Great Highway, a major north-south thoroughfare on San Francisco's western edge, was closed to vehicles from April 2020 to August 2021. The road was converted into a car-free active transportation route, with access permitted only to pedestrians and bicyclists. Vehicle traffic was rerouted to 19th Avenue, a portion of CA State Route 1 less than 3 km east of the Great Highway. In 2020, plants collected along these two roads had very similar $\Delta^{14}\text{C}$ values (0.8‰ difference, which is within the measurement uncertainty). In 2021, a plant collected on the Great Highway was still statistically indistinguishable from the 2020 samples (0.7‰ difference), while a plant sample collected on 19th Avenue was significantly more depleted relative to the 2020 sample (-24.8% difference, equivalent to an increase of 10 ppm C_{ff}). This indicates higher ffCO_2 emissions on 19th Avenue where traffic increased in 2021, while ffCO_2 emission reductions near the Great Highway persisted while the roadway remained closed to vehicles.

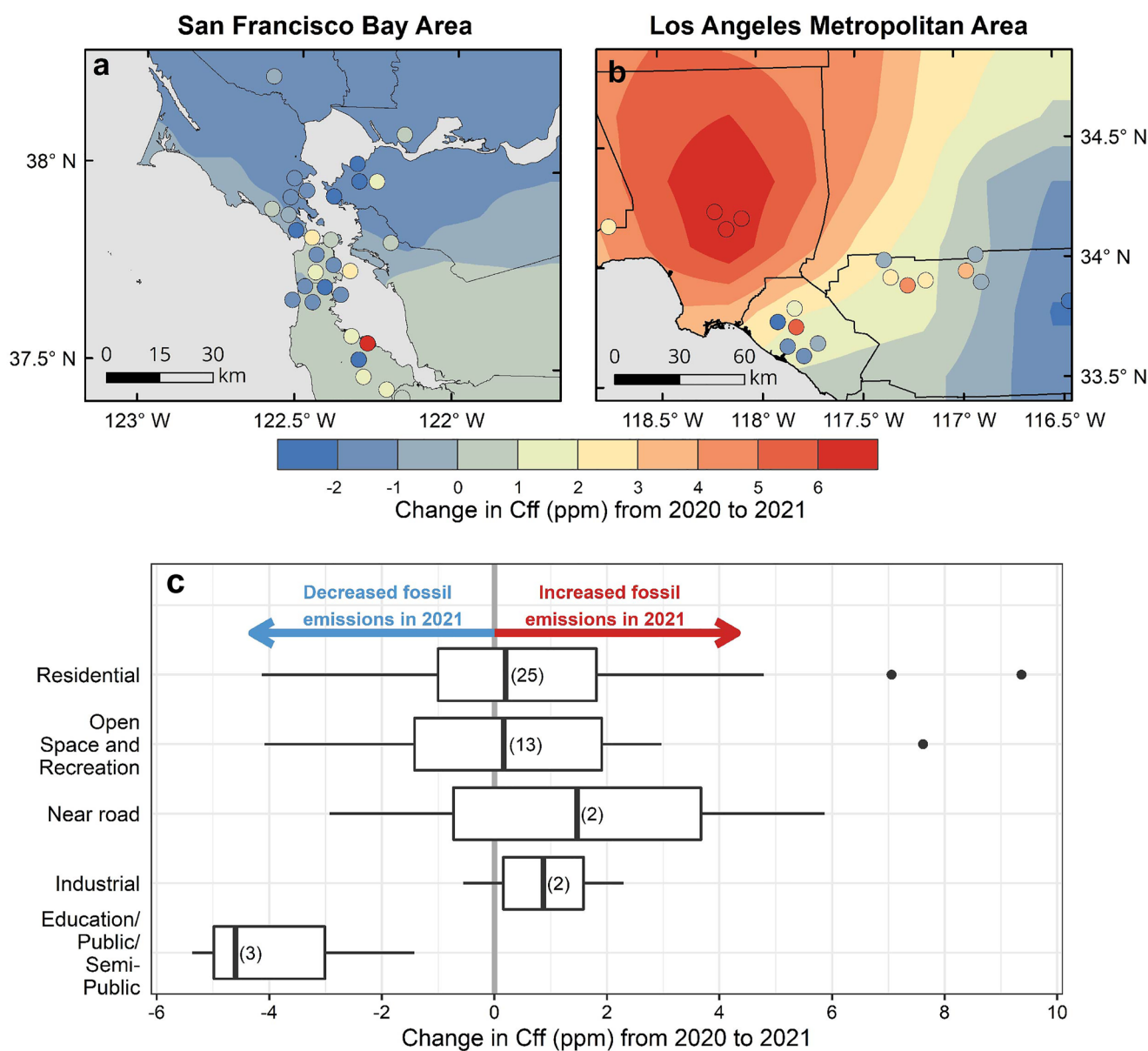


Figure 5. The difference in C_{ff} values from 2020 to 2021 between plant samples repeatedly collected in California's urban areas: (a) the San Francisco Bay Area and (b) the Los Angeles metropolitan area. Points show sample locations colored by their change in C_{ff} . Redder colors indicate $ffCO_2$ emission increases in 2021 compared to 2020. Background colors were calculated using an Ordinary Kriging interpolation of C_{ff} in ESRI's ArcMap software. C_{ff} changes by land use class are shown in (c).

All in all, we observed varying degrees of $ffCO_2$ reductions and rebound during the COVID-19 pandemic at various domains and spatiotemporal scales (Table 1). Year-to-year differences were more evident in urban domains (i.e., LA, Pasadena) than in statewide means or in coastal samples (e.g., Irvine).

3.4. Best Practices and Recommendations for Future Plant Radiocarbon Studies

Future work should conduct strategic experiments to better understand the correspondence between plant ^{14}C and other $ffCO_2$ atmospheric monitoring metrics. This will improve the applicability of plant ^{14}C analysis as a tool for monitoring decarbonization in cities around the world. Plant ^{14}C analysis reflected trends in ambient $\Delta^{14}CO_2$, with plant values having reasonable correspondence with air records from Irvine, CA and Pt. Barrow, AK (Figure 3). However, our plant ^{14}C -based results contrast with our on-road CO_{2xs} observations where we observed a return to pre-pandemic conditions by July 2021. This is because the two datasets represent different

emission sources and geographic regions. While the $\text{CO}_{2\text{xs}}$ data specifically represents the LA area's on-road sector, our plant samples are mainly representative of statewide residential, open space and recreational areas, which showed a more heterogeneous response to the lifting of COVID-related restrictions. No plant samples were collected within 500-m of the roads surveyed with the mobile observatory (Figure 1), so the two datasets were not directly comparable. A more strategic sampling approach could reveal the relationship between these two approaches and the capacity of plants to monitor changes in transportation-sector emissions.

The spatial sensitivity (“footprint”) of a plant is expected to be very localized (<100 m) but may vary for each sample depending on the local topography and air ventilation conditions. Previous work has shown that plants are predominantly influenced by emissions within 20–40 m (Lichtfouse et al., 2005; Turnbull et al., 2022). In contrast, atmospheric CO_2 measurements from rooftop/tower sites integrate signals over larger spatial scales (~10 km) since the inlet is higher above the ground (Kort et al., 2013). This makes tower sites well-suited for continuous monitoring of net ffCO_2 trends over an entire city using the CO_2 differential between a set of inflow- and outflow-representative sites. However, the localized spatial sensitivity of plants could be advantageous for studies seeking to investigate emissions at the neighborhood scale or from specific ffCO_2 sources (i.e., individual facilities or roads). Such analyses would require a strategic sampling design, targeting specific emission sources such as major roads (Turnbull et al., 2022). Without such targeted sampling, aggregated plant ^{14}C results in complex urban environments can be difficult to interpret since they represent highly local ffCO_2 emissions that may vary based on individual and immeasurable factors (i.e., human behaviors) within a neighborhood. With appropriately targeted sample pairs, however, plant ^{14}C can effectively reveal ffCO_2 reduction outcomes of local decarbonization measures (e.g., the Great Highway case described in Section 3.3). Plant-based monitoring of ffCO_2 emissions could also potentially be an appropriate proxy for exposure to co-emitted air pollutants such as from vehicle traffic and may be able to elucidate environmental justice concerns between neighborhoods. Future investigations are needed to assess this.

It is important to constrain the timing of carbon uptake as much as possible to distinguish spatially driven changes from temporal changes. Atmospheric $^{14}\text{CO}_2$ undergoes large temporal oscillations (Figure 5) with the amplitude and seasonality driven by the timing of ^{14}C production and descent into the troposphere, natural and anthropogenic CO_2 fluxes, and seasonal meteorology (wind and air mixing conditions). While the timing of flask sample collection is well-known, the timing of CO_2 uptake by plants is more uncertain. However, plant samples compensate for that by integrating over daytime hours of their photosynthetic period, hence, reducing significant short-term variability observed in flask samples (e.g., Miller et al., 2020) to yield a seasonal average ffCO_2 .

By sampling annual grasses, we have assumed that our $\Delta^{14}\text{C}$ analysis represents the growing season of these species in the region. We verified this assumption using downscaled remotely sensed observations of solar induced fluorescence (SIF, Figure S8 in Supporting Information S1) (Turner, Köhler, et al., 2020) from the TROPOMI instrument onboard the Sentinel-5 Precursor satellite. Using the date of maximum SIF observance to represent the timing of peak growth, we found that all senesced plants had peak growth dates from March to May. We also observed some temporal agreement between plant $\Delta^{14}\text{C}$ and ambient $\Delta^{14}\text{CO}_2$ measured in Irvine, CA (Figures S8 and S9 in Supporting Information S1), indicating potential applications of plant ^{14}C at the sub-seasonal scale. However, many $\Delta^{14}\text{C}$ values did not coincide with the Irvine trend and were more strongly driven by their distance to major roads (Figure S8c in Supporting Information S1), showing that the main driver of the samples' ^{14}C content is proximity to ffCO_2 emissions, with seasonality a secondary driver. SIF observations can help constrain the timing of plant growth for future studies to disentangle the spatial and temporal drivers of plant ^{14}C . Future studies could also potentially use purposely grown plants to monitor ffCO_2 (i.e., turfgrasses, Figure S9 in Supporting Information S1), and actively manage the growing period to the timing of interest, which would allow similar analyses at smaller time scales and for other times of the year besides the annual grass growing season.

4. Conclusions

We quantified changes in fossil fuel consumption during the COVID-19 pandemic when California implemented aggressive mitigation measures, that included Stay-At-Home and work-from-home orders, travel limitations, and experienced widespread economic shutdown. On-road surveys of excess CO_2 demonstrated a drastic but temporary reduction in ffCO_2 emissions on LA freeways, with only about half the typical ffCO_2 emissions in July of 2020 and a return to pre-pandemic levels by July 2021. The analysis of ^{14}C in annual plants also revealed

a measurable reduction in LA's ffCO₂ emissions in the spring of 2020 and 2021, indicated by a smaller offset between plant ¹⁴C and ¹⁴C of well-mixed northern hemispheric CO₂, and less variation in plant ¹⁴C compared to previous years.

Our complementary approaches captured the heterogeneous reality of mandated and voluntary movement restrictions in California during the pandemic. Our study focused on a region rich in high quality datasets (i.e., previous ¹⁴C records, a neighborhood scale bottom-up inventory, and an *in-situ* tower network) which allowed us to assess ffCO₂ emission reductions in the context of long-term trends. Mobile surveys can detect year-to-year differences in ffCO₂ trends from the on-road sector with high confidence, but further work is needed to relate on-road CO₂ enhancements to vehicle emissions and their drivers. Future research to constrain the spatial and temporal representation of periodically surveyed plants can support the tracking of decarbonization outcomes in cities and neighborhoods without investment in energy- and maintenance-demanding infrastructure. To account for the extreme variability of emissions sources in urban environments, however, plant-based ffCO₂ monitoring should focus on temporally-repeated sampling of active plants in well-ventilated areas in the direct vicinity of specific emission sources.

Conflict of Interest

The authors declare no conflicts of interest relevant to this study.

Data Availability Statement

The datasets of on-road CO₂ and plant radiocarbon are available in the Dryad public data repository and can be accessed via <https://doi.org/10.7280/D1F98G> (Yañez et al., 2022). The city land use datasets are administered by the Association of Bay Area Governments, the Metropolitan Transportation Commission, and the Southern California Association of Governments. These datasets are available in the public domain: <https://opendata.mtc.ca.gov/datasets> (Planned Land Use 2005); <https://gisdata-scag.opendata.arcgis.com/datasets> (2019 Annual Land Use Data set (ALU v.2019.2)).

Acknowledgments

The authors wish to thank all community scientists who submitted plant samples for this study and the Amigos de Bolsa Chica for helping with recruitment. Additionally, we thank A. Ocampo, C. Gurguis, V. Carranza, A. Odwuor, and C. Limón for their assistance with mobile surveys and W. M. Keck Carbon Cycle Accelerator Mass Spectrometer facility staff for supporting isotope analyses. We also thank A. Turner for his insight on this manuscript and for providing the down-scaled solar induced fluorescence data to support the analysis. C. C. Yañez received support for this work from the National Science Foundation Graduate Research Fellowship Program (DGE-1839285). We also acknowledge helpful comments from three anonymous reviewers and Editor E. Davidson.

References

- Alessio, M., Anselmi, S., Conforto, L., Improta, S., Manes, F., & Manfra, L. (2002). Radiocarbon as a biomarker of urban pollution in leaves of evergreen species sampled in Rome and in rural areas (Lazio—Central Italy). *Atmospheric Environment*, 36(34), 5405–5416. [https://doi.org/10.1016/s1352-2310\(02\)00409-0](https://doi.org/10.1016/s1352-2310(02)00409-0)
- Baker, C. J. (1996). Outline of a novel method for the prediction of atmospheric pollution dispersal from road vehicles. *Journal of Wind Engineering and Industrial Aerodynamics*, 65(1–3), 395–404. [https://doi.org/10.1016/s0167-6105\(97\)00058-5](https://doi.org/10.1016/s0167-6105(97)00058-5)
- Barth, M., & Boriboonsomsin, K. (2008). Real-world carbon dioxide impacts of traffic congestion. *Transportation Research Record*, 2058(1), 163–171. <https://doi.org/10.3141/2058-20>
- Buchwitz, M., Reuter, M., Noël, S., Bramstedt, K., Schneising, O., Hilker, M., et al. (2021). Can a regional-scale reduction of atmospheric CO₂ during the COVID-19 pandemic be detected from space? A case study for east China using satellite XCO₂ retrievals. *Atmospheric Measurement Techniques*, 14(3), 2141–2166. <https://doi.org/10.5194/amt-14-2141-2021>
- Bush, S. E., Hopkins, F. M., Randerson, J. T., Lai, C. T., & Ehleringer, J. R. (2015). Design and application of a mobile ground-based observatory for continuous measurements of atmospheric trace gas and criteria pollutant species. *Atmospheric Measurement Techniques*, 8(8), 3481–3492. <https://doi.org/10.5194/amt-8-3481-2015>
- Caltrans, California Department of Transportation. (2021). *Caltrans*. California Department of transportation. Performance Measurement System Data Source. Retrieved from <http://pems.dot.ca.gov/>
- Carranza, V., Biggs, B., Meyer, D., Townsend-Small, A., Thiruvankatachari, R. R., Venkatram, A., et al. (2022). Isotopic signatures of methane emissions from dairy farms in California's San Joaquin valley. *Journal of Geophysical Research: Biogeosciences*, 127(1), 1–15. <https://doi.org/10.1029/2021JG006675>
- Chevallier, F., Zheng, B., Broquet, G., Ciais, P., Liu, Z., Davis, S. J., et al. (2020). Local anomalies in the column-averaged dry air mole fractions of carbon dioxide across the globe during the first months of the coronavirus recession. *Geophysical Research Letters*, 47(22), e2020GL090244. <https://doi.org/10.1029/2020GL090244>
- Djuricin, S., Xu, X., & Pataki, D. E. (2012). The radiocarbon composition of tree rings as a tracer of local fossil fuel emissions in the Los Angeles basin: 1980–2008. *Journal of Geophysical Research*, 117(D12), D12302. <https://doi.org/10.1029/2011jd017284>
- Dlugokencky, E. J., Mund, J. W., Crotwell, A. M., Crotwell, M. J., & Thoning, K. W. (2021). Atmospheric carbon dioxide dry air mole fractions from the NOAA GML carbon cycle cooperative global air sampling network, 1968–2020, Version: 2021-07-30. <https://doi.org/10.1513/wkgl-f215>
- Duren, R. M., & Miller, C. E. (2012). Measuring the carbon emissions of megacities. In *Nature climate change* (Vol. 2(8), pp. 560–562). Nature Publishing Group. <https://doi.org/10.1038/nclimate1629>
- Fitzmaurice, H. L., Turner, A. J., Kim, J., Chan, K., Delaria, E. R., Newman, C., et al. (2022). Assessing vehicle fuel efficiency using a dense network of CO₂ observations. *Atmospheric Chemistry and Physics*, 22(6), 3891–3900. <https://doi.org/10.5194/acp-22-3891-2022>
- Gately, C. K., Hutyra, L. R., & Sue Wing, I. (2015). Cities, traffic, and CO₂: A multidecadal assessment of trends, drivers, and scaling relationships. *Proceedings of the National Academy of Sciences*, 112(16), 4999–5004. <https://doi.org/10.1073/pnas.1421723112>

- Gensheimer, J., Turner, A. J., Shekhar, A., Wenzel, A., Keutsch, F. N., & Chen, J. (2021). What are the different measures of mobility telling us about surface transportation CO₂ emissions during the COVID-19 pandemic? *Journal of Geophysical Research: Atmospheres*, *126*(11), 1–11. <https://doi.org/10.1029/2021JD034664>
- Graven, H., Keeling, R. F., & Rogelj, J. (2020). Changes to carbon isotopes in atmospheric CO₂ over the industrial era and into the future. *Global Biogeochemical Cycles*, *34*(11), 1–21. <https://doi.org/10.1029/2019GB006170>
- Gurney, K. R., Liang, J., Patarasuk, R., Song, Y., Huang, J., & Roest, G. (2020). The Vulcan version 3.0 high-resolution fossil fuel CO₂ emissions for the United States. *Journal of Geophysical Research: Atmospheres*, *125*(19), e2020JD032974. <https://doi.org/10.1029/2020jd032974>
- Gurney, K. R., Patarasuk, R., Liang, J., Song, Y., O'Keefe, D., Rao, P., et al. (2019). The Hestia fossil fuel CO₂ emissions data product for the Los Angeles megacity (Hestia-LA). *Earth System Science Data Discussions*, *11*(3), 1–38. <https://doi.org/10.5194/essd-2018-162>
- Harkins, C., McDonald, B. C., Henze, D. K., & Wiedinmyer, C. (2021). A fuel-based method for updating mobile source emissions during the COVID-19 pandemic. *Environmental Research Letters*, *16*(6), 065018. <https://doi.org/10.1088/1748-9326/ac0660>
- Hopkins, F. M., Kort, E. A., Bush, S. E., Ehleringer, J. R., Lai, C.-T., Blake, D. R., & Randerson, J. T. (2016). Spatial patterns and source attribution of urban methane in the Los Angeles basin. *Journal of Geophysical Research: Atmospheres*, *121*(5), 2490–2507. <https://doi.org/10.1002/2015JD024429>. Received
- Hsueh, D. Y., Krakauer, N. Y., Randerson, J. T., Xu, X., Trumbore, S. E., & Southon, J. R. (2007). Regional patterns of radiocarbon and fossil fuel-derived CO₂ in surface air across North America. *Geophysical Research Letters*, *34*(2), L02816. <https://doi.org/10.1029/2006gl027032>
- IPCC. (2022). Summary for policymakers. In P. R. Shukla, J., Skea, R., Slade, A., Al Khourdajie, R. van Diemen, et al. (Eds.), *Climate change 2022: Mitigation of climate change. Contribution of working group III to the sixth assessment report of the intergovernmental panel on climate change*. Cambridge University Press. <https://doi.org/10.1017/9781009157926.001>
- Kiel, M., Eldering, A., Roten, D. D., Lin, J. C., Feng, S., Lei, R., et al. (2021). Urban-focused satellite CO₂ observations from the orbiting carbon observatory-3: A first look at the Los Angeles megacity. *Remote Sensing of Environment*, *258*, 112314. <https://doi.org/10.1016/j.rse.2021.112314>
- Kort, E. A., Angevine, W. M., Duren, R., & Miller, C. E. (2013). Surface observations for monitoring urban fossil fuel CO₂ emissions: Minimum site location requirements for the Los Angeles megacity. *Journal of Geophysical Research: Atmospheres*, *118*(3), 1577–1584. <https://doi.org/10.1002/jgrd.50135>
- Le Quéré, C., Jackson, R. B., Jones, M. W., Smith, A. J. P., Abernethy, S., Andrew, R. M., et al. (2020). Temporary reduction in daily global CO₂ emissions during the COVID-19 forced confinement. *Nature Climate Change*, *10*, 1–7. <https://doi.org/10.1038/s41558-020-0797-x>
- Le Quéré, C., Peters, G. P., Friedlingstein, P., Andrew, R. M., Canadell, J. G., Davis, S. J., et al. (2021). Fossil CO₂ emissions in the post-COVID-19 era. *Nature Climate Change*, *11*(3), 197–199. <https://doi.org/10.1038/s41558-021-01001-0>
- Levin, I., Kromer, B., Schmidt, M., & Sartorius, H. (2003). A novel approach for independent budgeting of fossil fuel CO₂ over Europe by 14CO₂ observations. *Geophysical Research Letters*, *30*(23), 2194. <https://doi.org/10.1029/2003gl018477>
- Lichtfouse, E., Lichtfouse, M., Kashgarian, M., & Bol, R. (2005). 14C of grasses as an indicator of fossil fuel CO₂ pollution. *Environmental Chemistry Letters*, *3*(2), 78–81. <https://doi.org/10.1007/s10311-005-0100-4>
- Liu, D., Sun, W., Zeng, N., Han, P., Yao, B., Liu, Z., et al. (2021). Observed decreases in on-road CO₂ concentrations in Beijing during COVID-19 restrictions. *Atmospheric Chemistry and Physics*, *21*(6), 4599–4614. <https://doi.org/10.5194/acp-21-4599-2021>
- Liu, Z., Ciaia, P., Deng, Z., Lei, R., Davis, S. J., Feng, S., et al. (2020). Near-real-time monitoring of global CO₂ emissions reveals the effects of the COVID-19 pandemic. *Nature Communications*, *11*(1), 1–12. <https://doi.org/10.1038/s41467-020-18922-7>
- Maness, H. L., Thurlow, M. E., McDonald, B. C., & Harley, R. A. (2015). Estimates of CO₂ traffic emissions from mobile concentration measurements. *Journal of Geophysical Research: Atmospheres*, *120*(5), 2087–2102. <https://doi.org/10.1002/2014JD022876>
- Miller, J. B., Lehman, S. J., Verhulst, K. R., Miller, C. E., Duren, R. M., Yadav, V., et al. (2020). Large and seasonally varying biospheric CO₂ fluxes in the Los Angeles megacity revealed by atmospheric radiocarbon. *Proceedings of the National Academy of Sciences of the United States of America*, *117*(43), 26681–26687. <https://doi.org/10.1073/pnas.2005253117>
- Mitchell, L. E., Lin, J. C., Bowling, D. R., Pataki, D. E., Strong, C., Schauer, A. J., et al. (2018). Long-term urban carbon dioxide observations reveal spatial and temporal dynamics related to urban characteristics and growth. *Proceedings of the National Academy of Sciences of the United States of America*, *115*(12), 2912–2917. <https://doi.org/10.1073/pnas.1702393115>
- Newman, S., Xu, X., Affek, H. P., Stolper, E., & Epstein, S. (2008). Changes in mixing ratio and isotopic composition of CO₂ in urban air from the Los Angeles basin, California, between 1972 and 2003. *Journal of Geophysical Research*, *113*(D23), D23304. <https://doi.org/10.1029/2008jd009999>
- Newman, S., Xu, X., Gurney, K. R., Hsu, Y. K., Li, K. F., Jiang, X., et al. (2016). Toward consistency between trends in bottom-up CO₂ emissions and top-down atmospheric measurements in the Los Angeles megacity. *Atmospheric Chemistry and Physics*, *16*(6), 3843–3863. <https://doi.org/10.5194/acp-16-3843-2016>
- Nicolini, G., Antonielli, G., Carotenuto, F., Christen, A., Ciaia, P., Feigenwinter, C., et al. (2022). Direct observations of CO₂ emission reductions due to COVID-19 lockdown across European urban districts. *Science of the Total Environment*, *830*, 154662. <https://doi.org/10.1016/j.scitotenv.2022.154662>
- Oda, T., Haga, C., Hosomi, K., Matsui, T., & Bun, R. (2021). Errors and uncertainties associated with the use of unconventional activity data for estimating CO₂ emissions: The case for traffic emissions in Japan. *Environmental Research Letters*, *16*(8), 084058. <https://doi.org/10.1088/1748-9326/ac109d>
- Pickers, P. A., Manning, A. C., Le Quéré, C., Forster, G. L., Luijckx, I. T., Gerbig, C., et al. (2022). Novel quantification of regional fossil fuel CO₂ reductions during COVID-19 lockdowns using atmospheric oxygen measurements. *Science Advances*, *8*(16), eab19250. <https://doi.org/10.1126/sciadv.ab19250>
- Rao, P., Gurney, K. R., Patarasuk, R., Song, Y., Miller, C. E., Duren, R. M., & Eldering, A. (2017). Spatio-temporal variations in on-road CO₂ emissions in the Los Angeles megacity. *AIMS Geosciences*, *3*(2), 239–267. <https://doi.org/10.3934/geosci.2017.2.239>
- Riley, W. J., Hsueh, D. Y., Randerson, J. T., Fischer, M. L., Hatch, J. G., Pataki, D. E., et al. (2008). Where do fossil fuel carbon dioxide emissions from California go? An analysis based on radiocarbon observations and an atmospheric transport model. *Journal of Geophysical Research*, *113*(G4), G04002. <https://doi.org/10.1029/2007jg000625>
- Rosenzweig, C., Solecki, W., Hammer, S. A., & Mehrotra, S. (2010). Cities lead the way in climate-change action. *Nature*, *467*(7318), 909–911. <https://doi.org/10.1038/467909a>
- Santos, G. M., Oliveira, F. M., Park, J., Sena, A. C. T., Chiquetto, J. B., Macario, K. D., & Grainger, C. S. G. (2019). Assessment of the regional fossil fuel CO₂ distribution through Δ14C patterns in ipê leaves: The case of Rio de Janeiro state, Brazil. *City and Environment Interactions*, *1*, 100001. <https://doi.org/10.1016/j.cacint.2019.06.001>
- Schwandner, F. M., Gunson, M. R., Miller, C. E., Carn, S. A., Eldering, A., Krings, T., et al. (2017). Spaceborne detection of localized carbon dioxide sources. *Science*, *358*(6360). <https://doi.org/10.1126/science.aam5782>

- Seto, K. C., Dhakal, S., Bigio, A., Blanco, H., Delgado, G. C., De-war, D., et al. (2014). Human settlements, infrastructure, and spatial planning. In *Climate change 2014 mitigation of climate change. Contribution of working group III to the fifth assessment report of the intergovernmental panel on climate change* (pp. 923–1000). <https://doi.org/10.1017/cbo9781107415416.018>
- Sharma, R., Kunchala, R. K., Ojha, S., Kumar, P., Gargari, S., & Chopra, S. (2023). Spatial distribution of fossil fuel derived CO₂ over India using radiocarbon measurements in crop plants. *Journal of Environmental Sciences*, 124, 19–30. <https://doi.org/10.1016/j.jes.2021.11.003>
- Thiruvenkatachari, R. R., Carranza, V., Ahangar, F., Marklein, A., Hopkins, F., & Venkatram, A. (2020). Uncertainty in using dispersion models to estimate methane emissions from manure lagoons in dairies. *Agricultural and Forest Meteorology*, 290, 108011. <https://doi.org/10.1016/j.agrformet.2020.108011>
- Trumbore, S. E., Sierra, C. A., & Hicks Pries, C. E. (2016). Radiocarbon nomenclature, theory, models, and interpretation: Measuring age, determining cycling rates, and tracing source pools. *Radiocarbon and climate change* (pp. 45–82). https://doi.org/10.1007/978-3-319-25643-6_3
- Turnbull, J. C., Domingues, L. G., & Turton, N. (2022). Dramatic lockdown fossil fuel CO₂ decrease detected by citizen science-supported atmospheric radiocarbon observations. *Environmental Science & Technology*.
- Turnbull, J. C., Karion, A., Davis, K. J., Lauvaux, T., Miles, N. L., Richardson, S. J., et al. (2018). Synthesis of urban CO₂ emission estimates from multiple methods from the Indianapolis Flux Project (INFLUX). *Environmental Science and Technology*, 53(1), 287–295. <https://doi.org/10.1021/acs.est.8b05552>
- Turnbull, J. C., Karion, A., Fischer, M. L., Faloona, I., Guilderson, T., Lehman, S. J., et al. (2011). Assessment of fossil fuel carbon dioxide and other anthropogenic trace gas emissions from airborne measurements over Sacramento, California in spring 2009. *Atmospheric Chemistry and Physics*, 11(2), 705–721. <https://doi.org/10.5194/acp-11-705-2011>
- Turnbull, J. C., Miller, J. B., Lehman, S. J., Tans, P. P., Sparks, R. J., & Southon, J. (2006). Comparison of 14CO₂, CO, and SF₆ as tracers for recently added fossil fuel CO₂ in the atmosphere and implications for biological CO₂ exchange. *Geophysical Research Letters*, 33(1), L01817. <https://doi.org/10.1029/2005gl024213>
- Turner, A. J., Kim, J., Fitzmaurice, H., Newman, C., Worthington, K., Chan, K., et al. (2020). Observed impacts of COVID-19 on urban CO₂ emissions. *Geophysical Research Letters*, 47(22), 1–6. <https://doi.org/10.1029/2020GL090037>
- Turner, A. J., Köhler, P., Magney, T. S., Frankenberg, C., Fung, I., & Cohen, R. C. (2020). A double peak in the seasonality of California's photosynthesis as observed from space. *Biogeosciences*, 17(2), 405–422. <https://doi.org/10.5194/bg-17-405-2020>
- Vargas, R., Trumbore, S. E., & Allen, M. F. (2009). Evidence of old carbon used to grow new fine roots in a tropical forest (pp. 710–718).
- Verhulst, K. R., Karion, A., Kim, J., Salameh, P. K., Keeling, R. F., Newman, S., et al. (2017). Carbon dioxide and methane measurements from the Los Angeles megacity carbon Project – Part 1: Calibration, urban enhancements, and uncertainty estimates. *Atmospheric Chemistry and Physics*, 17(13), 8313–8341. <https://doi.org/10.5194/acp-17-8313-2017>
- Wang, W., & Pataki, D. E. (2010). Spatial patterns of plant isotope tracers in the Los Angeles urban region. *Landscape Ecology*, 25(1), 35–52. <https://doi.org/10.1007/s10980-009-9401-5>
- Ware, J., Kort, E. A., DeCola, P., & Duren, R. (2016). Aerosol lidar observations of atmospheric mixing in Los Angeles: Climatology and implications for greenhouse gas observations. *Journal of Geophysical Research: Atmospheres*, 121(16), 9862–9878. <https://doi.org/10.1002/2016JD024953>
- Xi, X., Ding, X., Fu, D., Zhou, L., & Liu, K. (2011). Regional $\Delta^{14}C$ patterns and fossil fuel derived CO₂ distribution in the Beijing area using annual plants. *Chinese Science Bulletin*, 56(16), 1721–1726. <https://doi.org/10.1007/s11434-011-4453-8>
- Xu, X., Trumbore, S. E., Zheng, S., Southon, J. R., McDuffee, K. E., Luttgren, M., & Liu, J. C. (2007). Modifying a sealed tube zinc reduction method for preparation of AMS graphite targets: Reducing background and attaining high precision. *Nuclear Instruments and Methods in Physics Research Section B: Beam Interactions with Materials and Atoms*, 259(1), 320–329. <https://doi.org/10.1016/j.nimb.2007.01.175>
- Yadav, V., Ghosh, S., Mueller, K., Karion, A., Roest, G., Gourdj, S., et al. (2021). The impact of COVID-19 on CO₂ emissions in the Los Angeles and Washington DC/Baltimore metropolitan areas. *Geophysical Research Letters*, 48(11), e2021GL092744. <https://doi.org/10.1029/2021GL092744>
- Yañez, C. C., Hopkins, F. M., Xu, X., Tavares, J. F., Welch, A. M., & Czimczik, C. I. (2022). Reductions in California's urban fossil fuel CO₂ emissions during the COVID-19 pandemic [Dataset]. Dryad. <https://doi.org/10.7280/D1F98G>
- Zheng, B., Geng, G., Ciais, P., Davis, S. J., Martin, R. V., Meng, J., et al. (2020). Satellite-based estimates of decline and rebound in China's CO₂ emissions during COVID-19 pandemic. *Science Advances*, 6(49). <https://doi.org/10.1126/sciadv.abd4998>
- Zhou, Y., Smith, S. J., Zhao, K., Imhoff, M., Thomson, A., Bond-Lamberty, B., et al. (2015). A global map of urban extent from nightlights. *Environmental Research Letters*, 10(5), 2000–2010. <https://doi.org/10.1088/1748-9326/10/5/054011>